International Journal of Applied Engineering Research ISSN 0973-4562 Volume 14, Number 10 (2019) pp. 2315-2326

A Fuzzy Logic Controlled Solar Power Generation with Integrated Maximum Power Point Tracking using Multi-level inverter

A.Ravi *, S.Murugan, Mr J. Daniel Sathiyaraj, Mrs R.Aandal

Department of Electrical and Electronics Engineering, Francis Xavier Engineering College, Tirunelveli, India.

** Corresponding Author*

Abstract

This paper presents a grid-connected photovoltaic (PV) power conversion system based on a new single-phase multilevel inverter and DC/DC converter. First, configuration and structural parts of the PV assisted inverter system are introduced in detail. This new seven level inverter comprises of capacitor selection circuit which is connected in cascade with full bridge power converter circuit. There are two output voltages in the capacitor selection circuit. Two output voltage sources of dc–dc power converter converts into a three-level dc voltage using capacitor selection circuit. The full-bridge power converter further converts this three-level dc voltage into a seven-level ac voltage. There are six power electronic switches in seven level inverter which simplifies the circuit configuration and losses. In this way, the proposed grid-connected PV power conversion system generates seven-level output voltage and a sinusoidal output current which is in-phase with the utility voltage and is fed into the grid. A digital PI current control algorithm is used to remain the current injected into the grid sinusoidal and to achieve high dynamic performance with low total harmonic distortion (THD). The simulations

Keywords: Multi-level inverter, Maximum power point tracking (MPPT), Total harmonic distortion (THD), Solar array

1. INTRODUCTION

In recent years, the world is increasingly experiencing a great need for extra energy resources so as to reduce dependence on conventional sources, and PV energy could be a solution to that need. Also photovoltaic PV generation has received special attention nowadays as one of the major energy sources of the future because of its flexible configuration, less fuel cost and eco-friendly nature discussed by Zhou et al (2010) PV systems are occasionally operated in stand-alone mode and they feed fixed loads by stand-alone PV inverters Saravana Ilango et al., (2010) PV systems are also interconnected to the grid. Various inverter topologies are presented, compared, and evaluated against demands, lifetime, component ratings, and cost Soeren Baekhoej Kjaer et al (2005). Interconnecting a PV system to the grid has been the fashionable design trend and grid-connection types of PV inverters have been projected by Calais et al., 1999; Lee et al.2008; Ersoy et al 2010 with single-phase multilevel inverter. Therefore various power electronics technologies are improved to convert the dc to ac power.

However, the output power induced in the PV modules depends on variation in temperature, irradiance, interior parameters and partial shading, etc; as discussed by Salameh et al (1999), Bader et al (2013). Therefore, only for one specific operating point, the maximum power output is obtained from the solar panel. The efficiency of the PV generation depends on maximum power extraction of PV system. The PV array has a distinctive operating point that can supply maximum power to the load as explained by Villalva et al (2009).The maximum power point of PV array is variation, so a search algorithm is given according to the (current-voltage) I-V and (power-voltage) P-V characteristics of the solar cell Kim et al (2008). To extract the maximum amount of power from the photovoltaic generator system an optimized perturb and observe MPPT technique which is carried out by using the as a benchmark reference has been reported by Femia et al (2009). Also Yu & Chien et al (2009) developed a photovoltaic simulation system with MPP tracking function using Matlab/Simulink software in order to simulate, evaluate and forecast the behaviours of photovoltaic system. They also modelled a PV system with different temperature and irradiance conditions, after that, a model of a photovoltaic system with MPP tracker, which was developed using DC-DC buck-boost converter with the P&O method, was then established and simulated.

Multilevel inverter topologies (MLIs) are increasingly being used in medium and high power applications due to their many advantages such as low power dissipation on power switches, low harmonic contents and low electromagnetic interference (EMI) outputs. The most common multilevel inverter topologies and control schemes have been reviewed in Ilhami Colak et al (2011). The most considerable of these types are the diode clamped multi-level inverter (DCMI), the flying capacitor multi-level inverter (FCMI), the cascaded H-Bridge multi-level inverter (CHBMI), the magnetic coupled and the full bridge with cascaded transformers inverters. More recently, various novel topologies for seven-level inverters have been proposed. For example, a single-phase seven-level grid-connected inverter has been developed for a PV system Rahim et al (2011).

The control structure of the grid-connected PV system is composed of two structure control

1. The MPPT control, whose main property is to extract the maximum power from the PV generator,
2. The inverter control,(i.e.) the main goal:
   i. To control the active and regulate the reactive power injected into the grid.
   ii. To control the DC bus voltage.
   iii. To ensure high quality of the injected power.

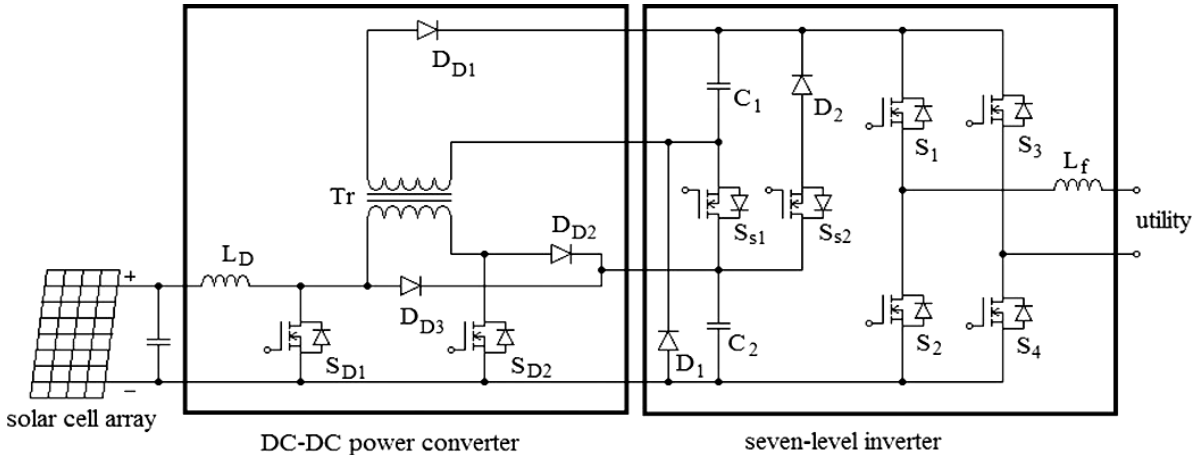

Fig.1. Configuration of the proposed solar power generation system

2. SYSTEM DESCRIPTION

The universal structure of the multilevel inverter is to synthesize a sinusoidal voltage from numerous levels of voltages, naturally obtained from capacitor voltage sources.

Fig. 1 shows the configuration of the proposed solar power generation system. The projected power generation structure is composed of a solar array, a DC–DC converter and a novel seven-level inverter. The solar array is connected to the DC–DC power converter. The DC-DC power converter is a boost converter that integrates a transformer with a turn ratio of 2:1. The DC-DC power converter converts the output power of the solar array into two autonomous voltage sources with multiple relationships, which are supplied to the seven-level inverter. This novel seven-level inverter is composed of a capacitor selection circuit and a full-bridge power converter, connected in a cascade. The power electronic switches of capacitor selection circuit determine the discharge of the two capacitors while the two capacitors are being discharged individually or in series. Because of the multiple relationships between the voltages of the DC capacitors, the capacitor selection circuit outputs a three-level DC voltage. The full-bridge power converter further converts this three-level DC voltage to a seven-level AC voltage that is synchronized with the utility voltage.

In this way, the proposed solar power generation system generates a sinusoidal output current that is in phase with the utility voltage and is fed into the utility, which produces a unity power factor. Since the novel seven-level inverter contains only six power electronic switches the power circuit is simplified.

3. PV ARRAY SIMULATION

The PV array used in the proposed system is KC200GT and it is simulated using a model based on Marcelo Gradella Villalva et al, (2009). In this model, a PV cell is represented by a current source in parallel with a diode and a series resistance as shown in Fig. 2. The basic current equation is given in (1)

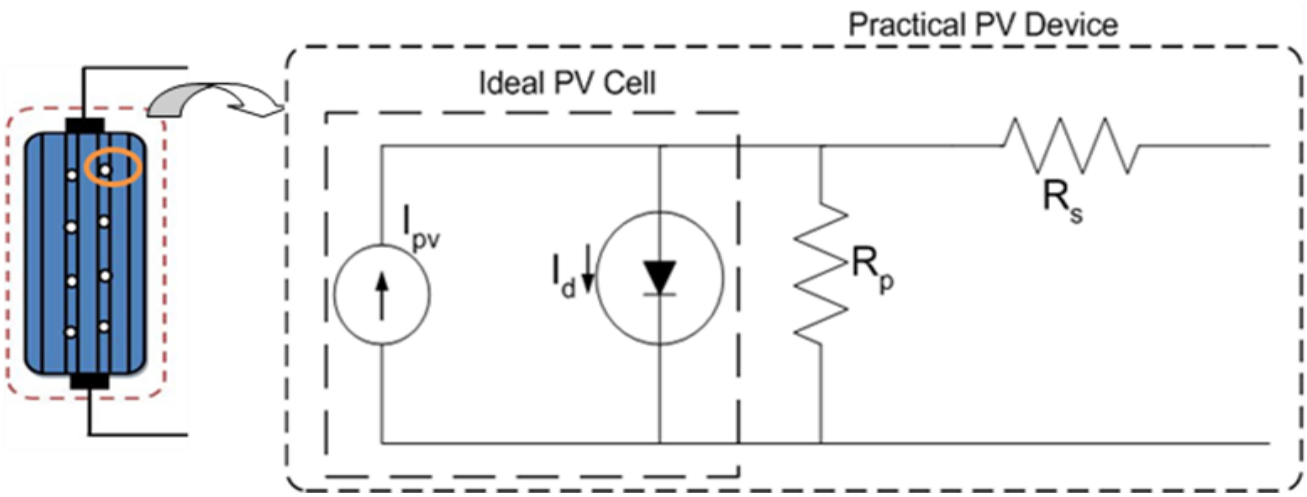

Fig. 2. Equivalent circuit of a PV Cell

$$I = I_{pv,cell} - I_{0,cell}\left[exp\frac{qv}{akT} - 1 \right] \quad (1)$$

where $I_{pv,cell}$ = current generated by the incident light (directly proportional to sun irradiation), $I_{0,cell}$ = leakage current of the diode, q = electron charge 1.60217646e10^{-19} C, k = Boltzmann constant, T = Temperature of the PN junction, a = Diode ideality constant.

But practically the PV array comprised with many PV cells connected in series and parallel connection. This makes some additional parameters to be added with the basic equation (1). The modified equation is shown in the equations (2) and (3).

$$I = I_{pv} - I_0\left[exp\left[\frac{V + R_s I}{V_t a} \right] - 1 \right] - \frac{V + R_s I}{R_p} \quad (2)$$

$$I_{pv} = \left(I_{pv,n} + K_I \Delta T\right)\frac{G}{G_n} \quad (3)$$

The parameters of solar array KC200GT at nominal operating conditions is shown in the Table 1 and the current-voltage and power-voltage characteristics are shown in Fig.3.

Table 1. Parameters of the adjusted model of the KC200GT solar array at nominal operating conditions

I_{mp}	7.61A
V_{mp}	26.3V
$P_{max,m}$	200.143W
I_{sc}	8.21A
V_{oc}	32.9V
$I_{o,n}$	9.825 *10^{-8} A
I_{pv}	8.214A
A	1.3
R_p	415.405Ω
R_s	0.221Ω

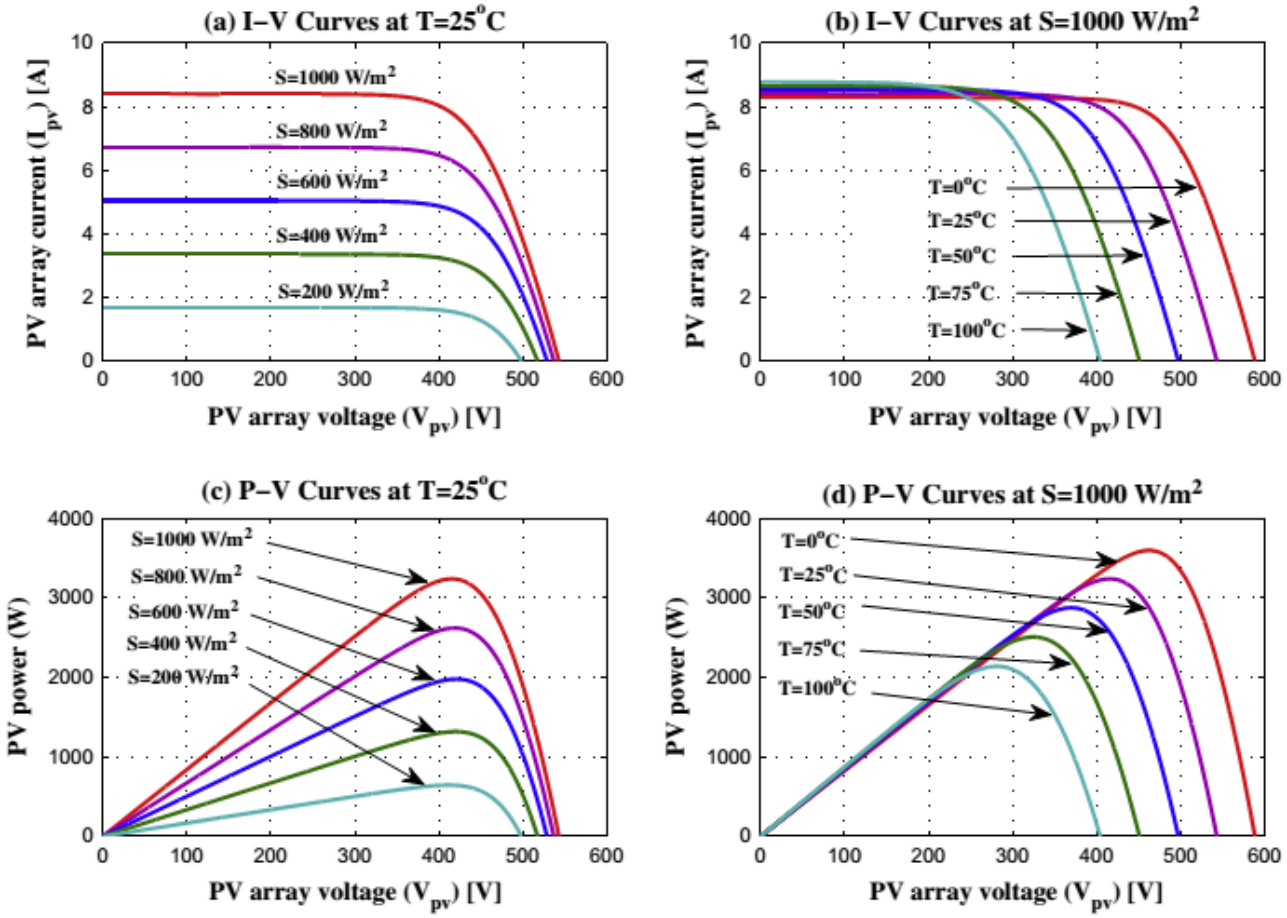

Fig.3. Current-voltage and power-voltage characteristics of PV array

4. FUZZY MPPT

Conventional methods of MPPT are based on load line adjustment under varying atmospheric and load conditions. However, these uncertainties make MPPT less suitable for rapidly changing environmental conditions or parameter variations. The fuzzy logic controller overcomes the problem of fluctuation of MPP around the operating point in perturbation and observation method (P&O) discussed Shiqiong Zhou et al (2010). Fuzzy logic controllers (FLCs) are coming up in industrial processes owing to their heuristic nature associated with simplicity and effectiveness for both linear and nonlinear systems. Fuzzy Logic has also been implemented in Ravi et al (2011). The control inputs to the FLC are voltage error and change of errors, while the output is the change of control signal for PWM generator. Use of FLCs for the PV systems will relieve the burden involved in the design of controller parameters. In addition to this, these controllers will improve the tracking performance as compared with conventional controllers.

The operation of this technique is explained in the block diagram shown in Fig. 4. The use of fuzzy logic control has become popular over the last decade because it can deal with imprecise inputs, does not need an accurate mathematical model and can handle nonlinearity.

The fuzzy logic consists of three stages: fuzzification, inference system and defuzzification. Fuzzification comprises the process of transforming numerical crisp inputs into linguistic variables based on the degree of membership to certain sets. Membership functions, like the ones in Fig. 4 are used to associate a grade to each linguistic term.

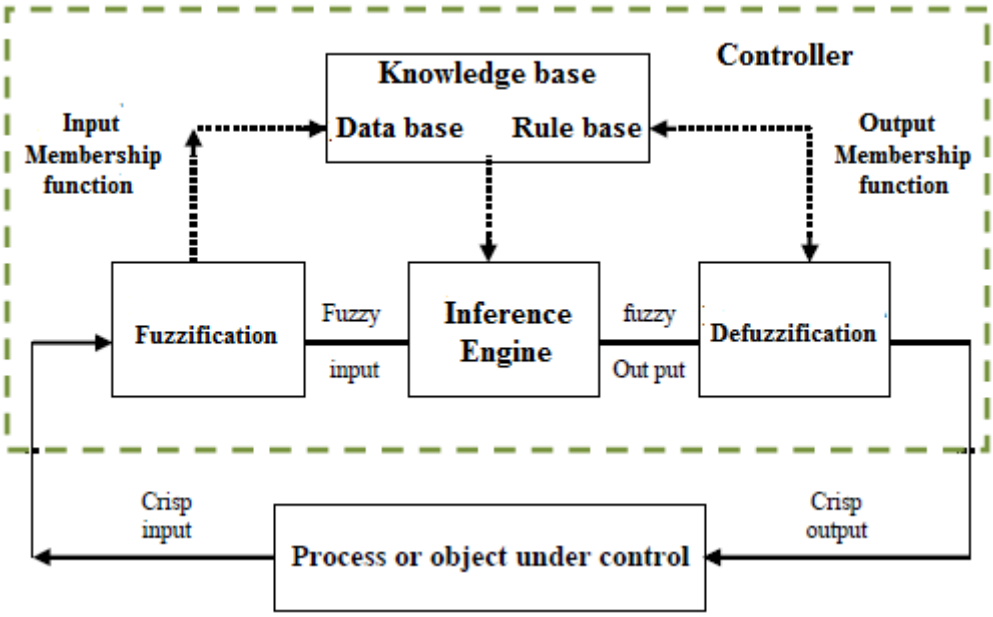

Fig. 4 Fuzzy logic systems

The number of membership functions used depends on the accuracy of the controller, but it usually varies between 5 and 7 discussed Esram et al 2007& S. Jain et al 2007. In Fig. 4 Five fuzzy levels are used: NB (Negative Big), NS (Negative Small), ZE (Zero), PS (Positive Small), and PB (Positive Big). The values *a*, *b* and *c* are based on the range values of the numerical variable. In some cases the membership functions are chosen less symmetric or even optimized for the application for better accuracy. In this work the fuzzy inference rule is carried out by using Mamdani's method. In accordance with Table 2, if the power (P_{pv}) increased, the operating point should be increased as well. FLC uses change in PV array Power (ΔP_{in}) and change in PV array voltage (ΔV_{in}) corresponding to the two sampling time instants to determine the duty cycle of converter.

Table 2. Fuzzy rule table

E/ΔE	**NB**	**NS**	**ZE**	**PS**	**PB**
NB	NB	NB	NS	NS	ZE
NS	NB	NS	NS	ZE	PS
ZE	NS	NS	ZE	PS	PS
PS	NS	ZE	PS	PS	PB
PB	ZE	PS	PS	PB	PB

Here, the insolation level (G) is altered from 800 to 600 W/m^2 at 0.008 s and then altered from 600 to 1000 W/m^2 at 0.015 s. The FLC uses a rule base as shown in Table 2 and the membership function as shown in Fig. 5. The tracking of maximum power of a PV system by using FLC is shown in Fig. 6. It can be seen that the FLC tracks the operating point very quickly and faster than other MPPT techniques.

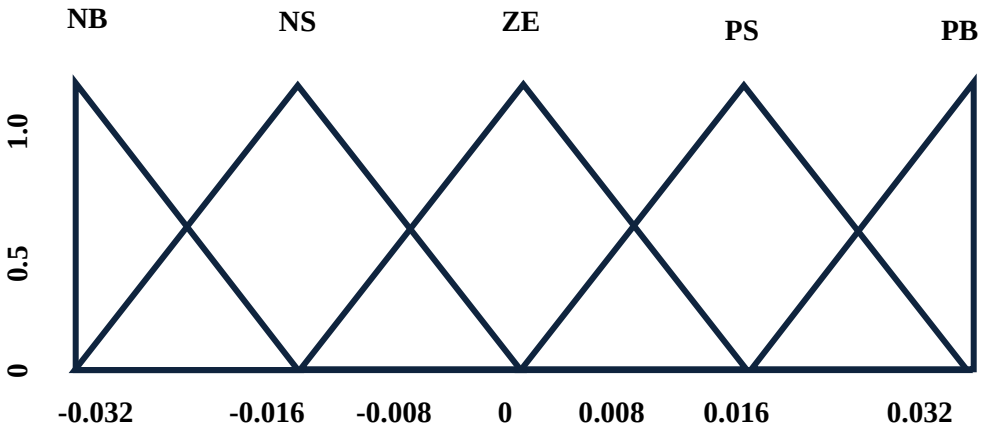

Fig.5. Fuzzy input and output membership function

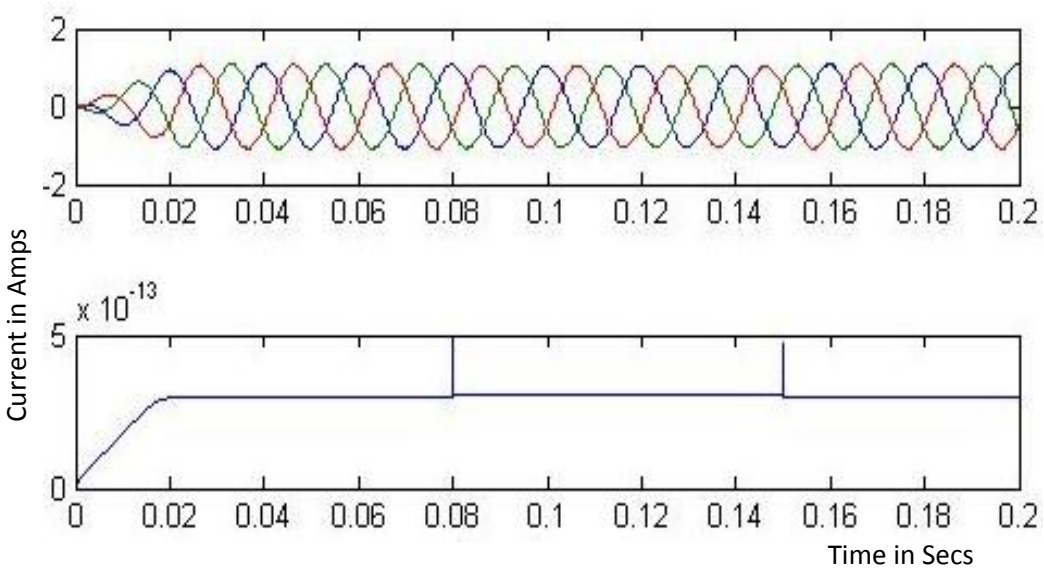

Fig. 6. MPPT tracking with output current

5. SEVEN LEVEL INVERTER TOPOLOGY

In Fig. 1, the seven-level inverter is composed of a capacitor selection circuit and a full-bridge power converter, which are connected in cascade. The function of the seven-level inverter can be separated into the positive half cycle and the negative half cycle of the utility. For ease of analysis, the power electronic switches and diodes are assumed to be ideal, while the voltages of both capacitors C_1 and C_2 in the capacitor selection circuit are constant and equal to $V_{dc}/3$ and $2V_{dc}/3$, respectively. Since the output current of the solar power generation system will be controlled to be sinusoidal and in phase with the utility voltage, the output current of the seven-level inverter is also positive in the positive half cycle of the utility. The operation of the seven-level inverter in the positive half cycle of the utility can be further divided into four modes, as shown in Fig. 7.

Mode 1: At this mode, the output voltage of the seven-level inverter is directly equal to the output voltage of the capacitor selection circuit, which means the output voltage of the seven-level inverter is $V_{dc}/3$.The operation is shown in Fig. 7(a). Both the capacitor selection switches S_{S1} and S_{S2} are OFF, so C_1 is discharged through D_1 and the output voltage of the capacitor selection circuit is $V_{dc}/3$. S_1 and S_4 of the full-bridge power converter are ON.

Mode 2: The operation of mode 2 is shown in Fig. 7(b). In the capacitor selection circuit, S_{S1} is OFF and S_{S2} is ON, so C_2 is discharged through S_{S2} and D_2 and the output voltage of the capacitor selection circuit is $2V_{dc}/3$. S_1 and S_4 of the full-bridge power converter are ON. At this point, the output voltage of the seven-level inverter is $2V_{dc}/3$.

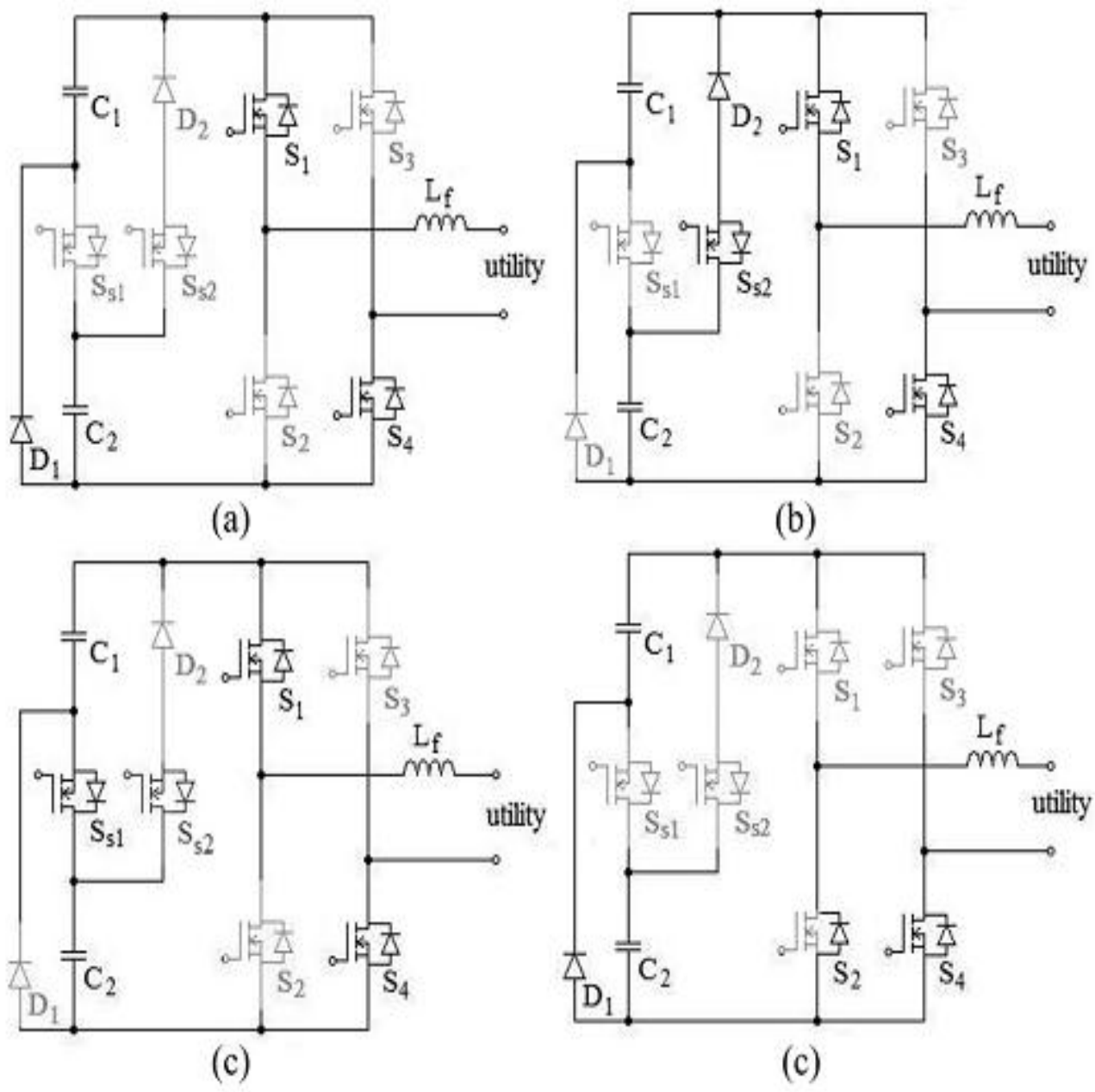

Fig. 7. Operation of the seven-level inverter in the positive half cycle, (a) mode 1, (b) mode 2, (c) mode 3, and (d) mode 4.

Mode 3: In this mode (shown in Fig. 7(c)) the capacitor selection circuit, S_{S1} is

ON. Since D_2 has a reverse bias when S_{S1} is ON, the state of S_{S2} cannot affect the current flow. Hence, S_{S2} may be ON or OFF, to keep away from switching of S_{S2}. Both C_1 and C_2 are discharged in series and the output voltage of the capacitor selection circuit is V_{dc}. S_1 and S_4 of the full-bridge power converter are ON. At this point, the output voltage of the seven-level inverter is V_{dc}.

Mode 4: The operation of mode 4 is shown in Fig. 7(d). Both S_{S1} and S_{S2} of the capacitor selection circuit are OFF. The output voltage of the capacitor selection circuit is $V_{dc}/3$. Only S_4 of the full-bridge power converter is ON. Since the output current of the seven-level inverter is positive and passes through the filter inductor, it forces the anti-parallel diode of S_2 to be switched ON for continuous conduction of the filter inductor current. At this point, the output voltage of the seven-level inverter is zero.

Therefore, in the positive half cycle, the output voltage of the seven-level inverter has four levels: V_{dc} ,$2V_{dc}/3$,$V_{dc}/3$ and 0. In the negative half cycle, the output current of the seven-level inverter is negative. The operation of the seven-level inverter can also be further divided into four modes, as shown in Fig. 8.

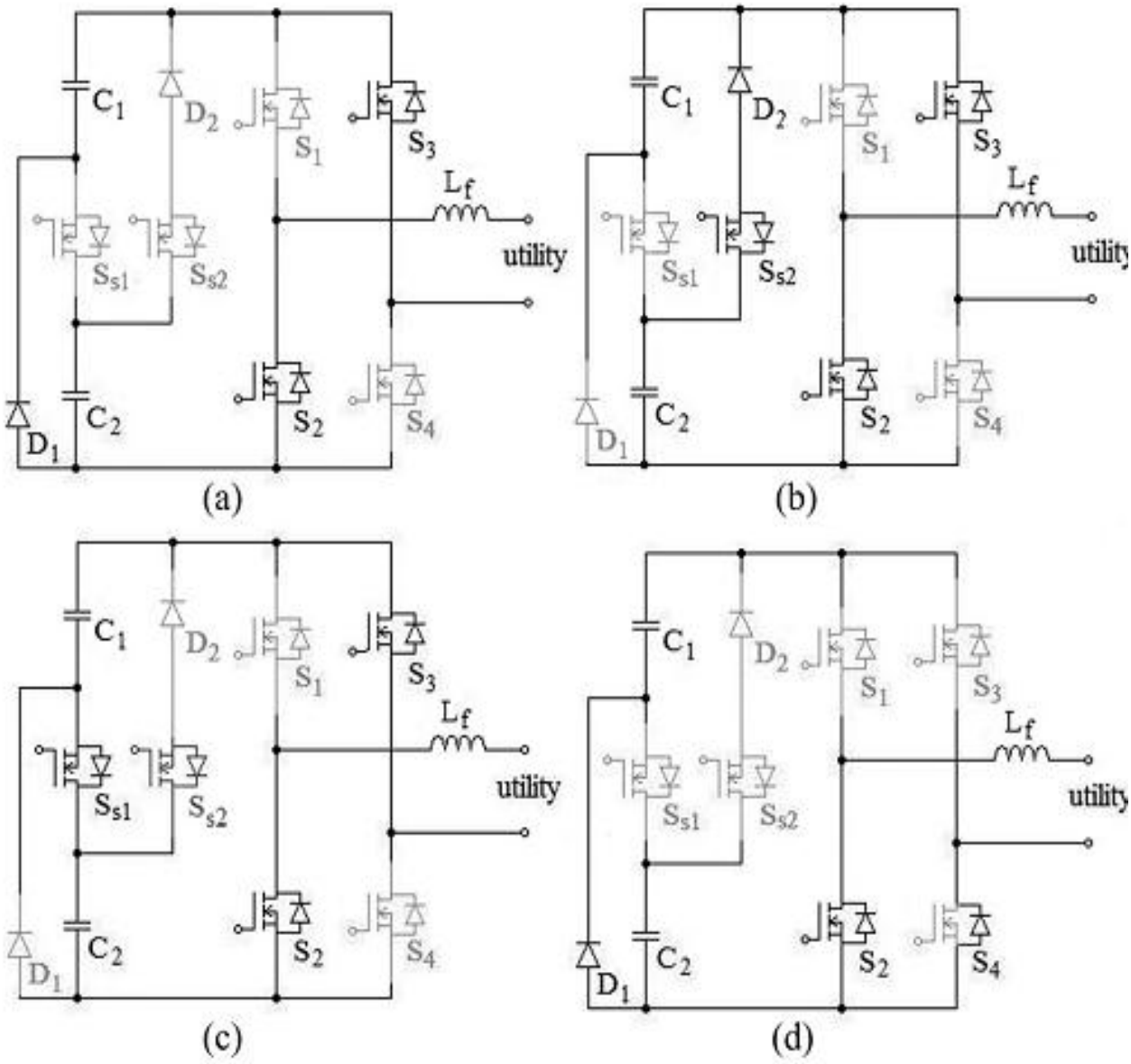

Fig. 8. Operation of the seven-level inverter in the negative half cycle: (a) mode 5, (b) mode 6, (c) mode 7, and (d) mode 8.

A comparison with Fig. 7 shows that the operation of the capacitor selection circuit in the negative half cycle is the same as that in the positive half cycle. The difference is that S_2 and S_3 of the full-bridge power converter are ON during modes 5, 6, and 7, and S_2 is also ON during mode 8 of the negative half cycle. Accordingly, the output voltage of the capacitor selection circuit is inverted by the full-bridge power converter, so the output voltage of the seven-level inverter also has four levels: $-V_{dc}$, $-2V_{dc}/3$, $-V_{dc}/3$, and 0.In summary, the output voltage of the seven-level inverter has the voltage levels: V_{dc} ,$2V_{dc}/3$,$V_{dc}/3$, 0,$-V_{dc}/3$,$-2V_{dc}/3$, and $-V_{dc}$.

The seven-level inverter is controlled by the current-mode control, and pulse-width modulation (PWM) is use to generate the control signals for the power electronic switches. The output voltage of the seven-level inverter must be switched in two levels, according to the utility voltage. One level of the output voltage is higher than the utility voltage in order to increase the filter inductor current, and the other level of the output voltage is lower than the utility voltage, in order to decrease the filter inductor current. In this way, the output current of the seven-level

6. CONTROL BLOCKS

a. DC-DC power converter

Fig. 9 shows the control block diagram for the DC–DC power converter. The output of solar cell array is fed as a input to DC-DC power converter. The MPPT function is degraded if the output voltage of solar cell array contains a ripple voltage. Therefore, the ripple voltages in C_1 and C_2 must be blocked by the DC–DC power converter to provide improved MPPT.

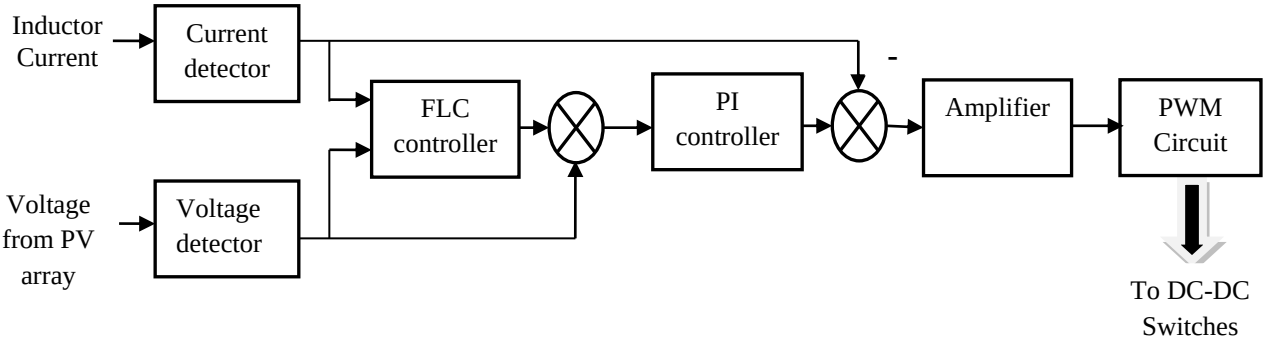

Fig. 9. Control block for DC-DC converter

Accordingly, dual control loops, an outer voltage control loop and an inner current control loop, are used to control the dc–dc power converter. Since the output voltages of the DC-DC power converter comprises the voltages of C1andC2, which are controlled by the seven-level inverter, the outer voltage control loop is used to regulate the output voltage of the solar cell array. The inner current control loop controls the inductor current so that it approaches a constant current and blocks the ripple voltages inC1 and C2. The output voltage of the solar cell array and the inductor current are detected and sent to a MPPT controller to determine the desired output voltage for the solar cell array. Then the detected output voltage and the desired output voltage of the solar cell array are sent to a subtractor and the difference is sent to a PI controller.

The output of the PI controller is the reference signal of the inner current control loop. The reference signal and the detected inductor current are sent to a subtractor and the difference is sent to an amplifier to complete the inner current control loop. The output of the amplifier is sent to the PWM circuit. The PWM circuit generates a set of complementary signals that control the power electronic switches of the DC–DC power converter.

b. Inverter control

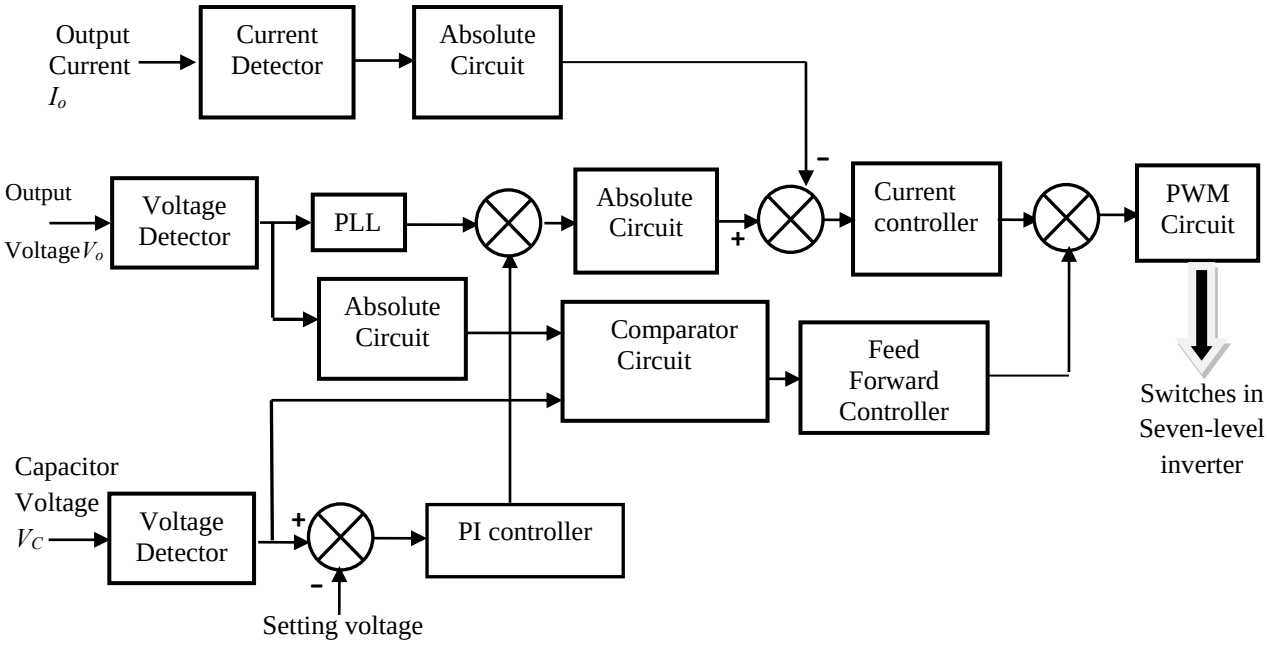

Fig.10 Control block for seven level inverter

Fig. 10 shows the control block diagram for the seven-level inverter. The control object of the seven-level inverter is its output current, which should be sinusoidal and in phase with the utility voltage. The utility voltage is detected by a voltage detector, and then sent to a phase-lock loop (PLL) circuit in order to generate a sinusoidal signal with unity amplitude. The voltage of capacitorC2 is detected and then compared with a setting voltage. The compared result is sent to a PI controller.

Then, the outputs of the PLL circuit and the PI controller are sent to a multiplier to produce the reference signal, while the output current of the seven-level inverter is detected by a current detector. The reference signal and the detected output current are sent to absolute circuits and then sent to a subtractor, and the output of the subtractor is sent to a current controller. The detected utility voltage is also sent to an absolute circuit and then sent to a comparator circuit, where the absolute utility voltage is compared with both half and whole of the detected voltage of capacitor C_2, in order to determine the range of the operating voltage. The comparator circuit has three output signals, which correspond to the operation voltage ranges, $(0, V_{dc}/3)$, $(V_{dc}/3,\ 2V_{dc}/3)$, and $(2V_{dc}/3, V_{dc})$.

Table 3. States of power electronic switches for a seven-level inverter

		Switches					
Output cycle	**Output voltage**	S_{S1}	S_{S2}	S_1	S_2	S_3	S_4
Positive half cycle	$V_o < V_{dc}/3$	0	0	PWM	0	0	1
	$2V_{dc}>Vo>V_{dc}/3$	0	PWM	1	0	0	1
	$V_o >2 V_{dc}/3$	PWM		1	0	0	1
Negative half cycle	$V_o < V_{dc}/3$	0	0	0	1	PWM	0
	$2V_{dc}>Vo>V_{dc}/3$	0	PWM	0	1	1	0
	$V_o >2 V_{dc}/3$	PWM	1	0	1	1	0

Then, the output of the current controller and the feed-forward signal are summed and sent to a PWM circuit to produce the PWM signal. The detected utility voltage is also compared with zero, in order to obtain a square signal that is synchronized with the utility voltage. Finally, the PWM signal, the square signal and the outputs of the compared circuit are sent to the switching signal processing circuit to generate the control signals for the power electronic switches of the seven-level inverter, according to Table.3 and control pulses for the switches are shown in Fig.11.

7. SIMULATION OUTPUT

To verify the presentation of the projected solar power generation system, a trial product was developed with a controller based on the DSP chip TMS320F28035. The power rating of the prototype is 500 W and the prototype was used for a single-phase utility with 220 V and 50 Hz.

Fig. 12 shows the Simulation results for the seven-level inverter when the output power of solar power generation system is 500 W. Fig.13 shows the experimental results for the AC side of the seven-level inverter. The output current of the seven-level inverter, shown in Fig. 14, is sinusoidal and in phase with the utility voltage, which means that the grid-connected power conversion interface feeds a pure real power to the utility. The total harmonic distortion (THD) of the output current of the seven-level inverter is 4.72% as shown in Fig.15.

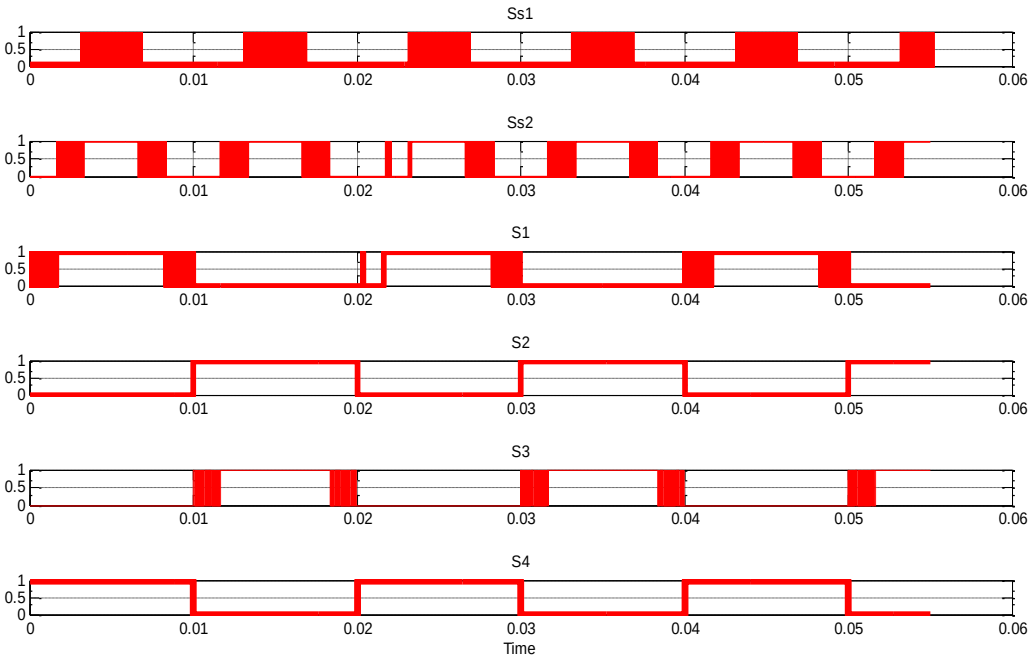

Fig.11. Control pulses for the converter switches

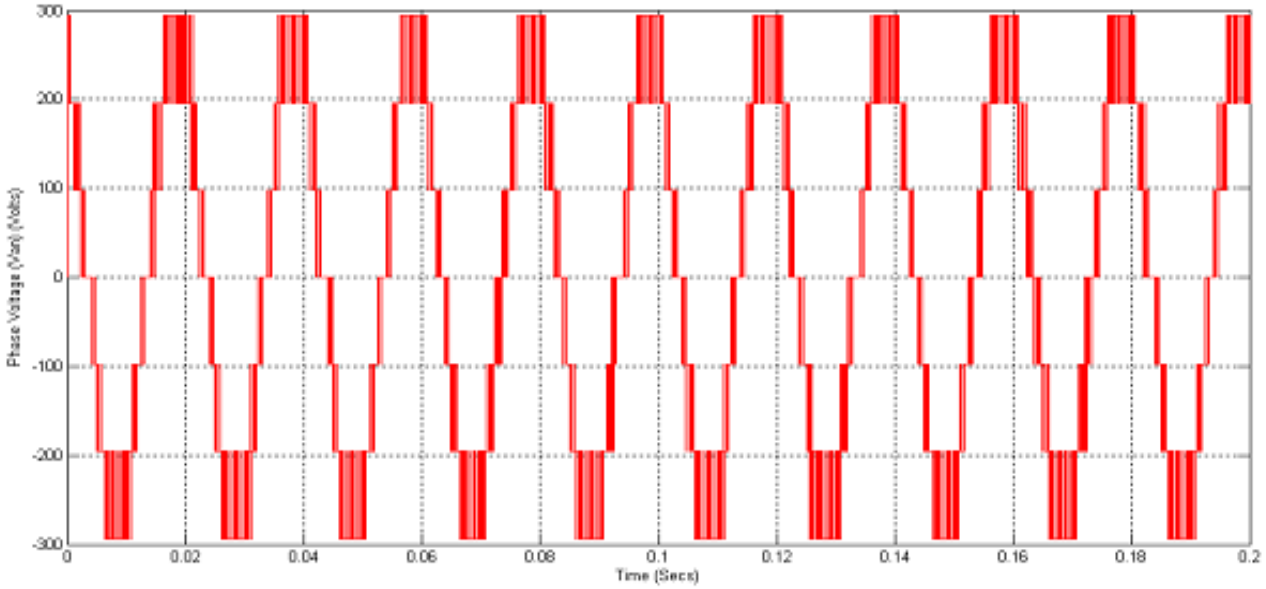

Fig.12. Simulation output voltage of novel seven-level inverter

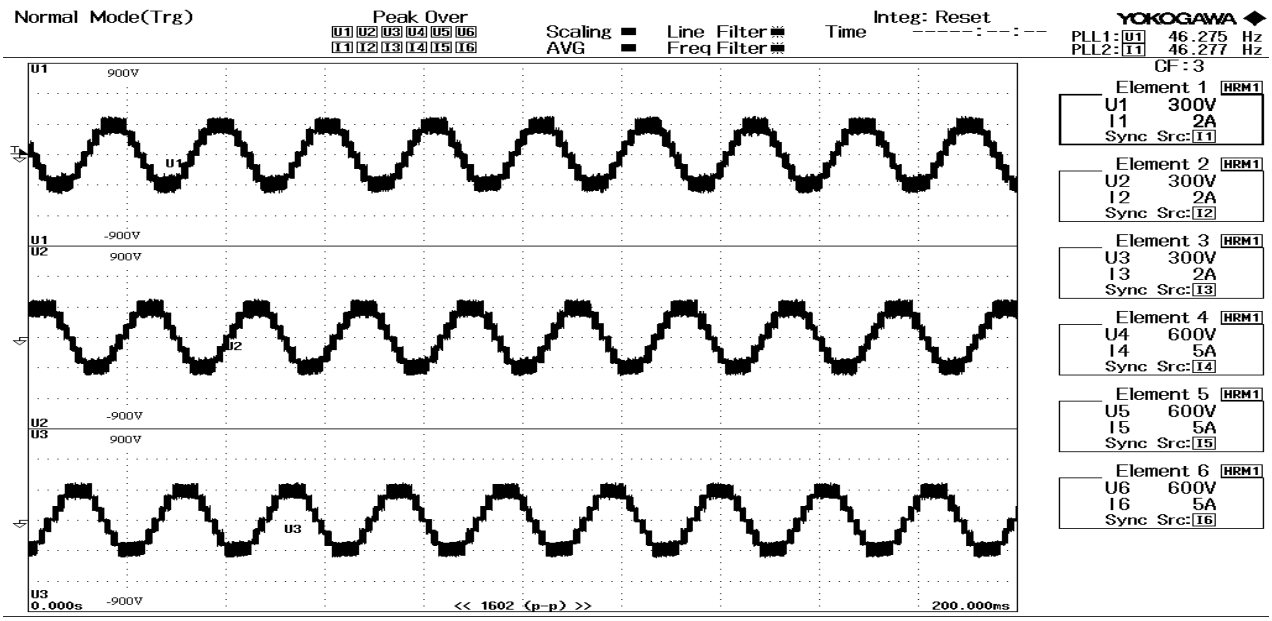

Fig.13. Experimental output voltage of novel seven-level inverter

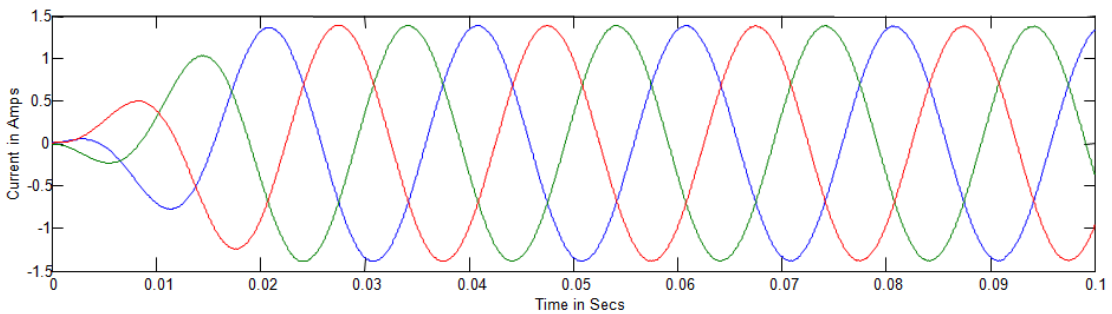

Fig.14. Output current of the seven-level inverter

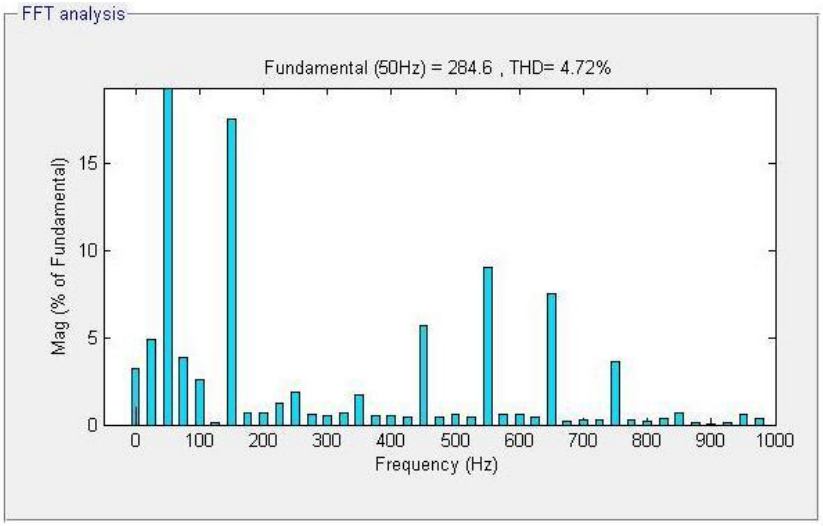

Fig.15. THD of seven-level inverter

8. CONCLUSION

This paper proposes a solar power generation system to convert the dc energy generated by a solar cell array into ac energy that is fed into the utility. The proposed solar power generation system is composed of a dc–dc power converter and a seven-level inverter. The seven-level inverter contains only six power electronic switches, which simplifies the circuit configuration. Furthermore, only one power electronic switch is switched at high frequency at any time to generate the seven-level output voltage. This reduces the switching power loss and improves the power efficiency. The voltages of the two dc capacitors in the proposed seven-level inverter are balanced automatically, so the control circuit is simplified. Experimental results show that the proposed solar power generation system generates a seven-level output voltage and outputs a sinusoidal current that is in phase with the utility voltage, yielding a power factor of unity. In addition, the proposed solar power generation system can effectively trace the maximum power of solar cell array.

REFERENCES

[1] Zhou S, Kang L, Sun J, Guo G, Cheng B, Cao B, Tang, Y, 2010 “A novel maximum power point tracking algorithms for stand-alone photovoltaic system”. Int J Control Autom System vol 8 no.6, pp1364.

[2] Saravana Ilango, G., Srinivasa Rao, P., Karthikeyan, A., Nagamani, C., 2010 “Single-stage sine-wave inverter for an autonomous operation of solar photovoltaic energy conversion system”. Renewable Energy 35(1), 275–282.

[3] Soeren Baekhoej Kjaer, John K. Pedersen, and Frede Blaabjerg 2005 “A Review of Single-Phase Grid-Connected Inverters for Photovoltaic Modules”. IEEE Transactions on industry applications, Vol. 41, No. 5. 1292-1306.

[4] Calais, M., Agelidis, V.G., Meinhardt, M., “Multilevel converters for single-phase grid connected photovoltaic systems: an overview”. Solar Energy 66 (5), 325–335. 1999.

[5] Lee, S.-H., Song, S.-G., Park, S.-J., Moon, C.-J., Lee, M.-H., 2008 “Grid connected photovoltaic system using current-source inverter”. SolarEnergy 82 (5), 411–419.

[6] Ersoy Beser, Birol Arifoglu, Sabri Camur, Esra Kandemir Beser 2010 “A grid-connected photovoltaic power conversion system”, solar Energy 84 2056-2067.

[7] Salameh, Z & Taylor, D, 1990 “step-up maximum power point tracker for photovoltaic arrays”, Solar Energy, vol.44, no.1, pp.57-61.

[8] Bader, N, Alajmi, Ahmed, Stephen, J, Finney, Barry,W & Williams, 2011 “Fuzzy logic control approach of a modified hill climbing method for maximum power point in microgrid standalone photovoltaic system”, IEEE Transactions on Power Electronics, vol.26, pp.1022-1030.

[9] Villalva, MG, Gazoli, JR & Filho, ER, 2009 “Comprehensive approach to modeling and simulation of photovoltaic arrays”, IEEE Transactions on Power Electronics, vol. 24, no. 5, pp. 1198-1208.

[10] Kim SK, Jeon JH, Cho CH, Ahn JB, Kwon SH. 2008 “Dynamic modeling and control of a grid-connected hybrid generation system with versatile power transfer”, IEEE Trans Ind Electron 55(4):73-82.

[11] Yu, TC, & Chien, TS 2009 “Analysis and simulation of characteristics and maximum power point tracking for photovoltaic systems”, International Conference on Power Electronics and Drive Systems, pp. 1339-1344.

[12] N. A. Rahim, K. Chaniago, and J. Selvaraj, 2011"Single-phase seven-level grid-connected inverter for photovoltaic system," IEEE Transaction on Industrial Electronics, vol. 58, no. 6, pp. 2435–2443.

[13] Marcelo Gradella Villalva, Jonas Rafael Gazoli, and Ernesto Ruppert Filho, 2009 "Comprehensive approach to modeling and simulation of photovoltaic arrays", IEEE Transactions On Power Electronics, 24 (5), 1198 – 1208.

[14] Shiqiong Zhou, Longyun Kang, Jing Sun, Guifang Guo, Bo Cheng, Binggang Cao & Yiping Tang, 2010 "A novel maximum power point tracking algorithms for stand-alone photovoltaic system", Internation Journal of Control Automation, Systems, vol.8, no.6, pp.1364-1371.

[15] Ravi.A, P.S.Manoharan, J.V,Anand, 2011 "Modeling and simulation of three phase multi-level Inverter For grid connected photovoltaic systems" solar energy. Vol.85, no.11, pp. 2811-2818.

[16] A.Ravi, 2012 "Harmonic Reduction of three-phase Multilevel Inverter for Grid Connected Photovoltaic System using Closed Loop Switching Control," International Review of Modelling and Simulations, Vol. 5 N. 5- PartA.

[17] A.Ravi, PS Manoharan, 2013 "Closed loop control of diode clamped multi-level inverter with integrated maximum power point tracking for grid connected photovoltaic application" Przegląd Elektrotechniczny, vol.10, pp.230-236.

[18] M Valan Rajkumar, PS Manoharan, A Ravi, 2013, "Simulation and an experimental investigation of SVPWM technique on a multi-level voltage source inverter for photovoltaic systems" , Electrical Power and Energy Systems, vol.52, pp. 116–131.

[19] KS Gobisha, Monica Shalini , A Ravi., 2015, "A Fuzzy logic Controlled Solar power Generation with Seven level Inverter," .International Journal of Emerging Technology and Advanced Engineering, volume 5, Issue 2 PP.285-288.

[20] Ning, X., and Lovell, M. R., 2002, "On the Sliding Friction Characteristics of Unidirectional Continuous FRP Composites," ASME J. Tribol., 124(1), pp. 5-13.

[21] Barnes, M., 2001, "Stresses in Solenoids," J. Appl. Phys., 48(5), pp. 2000–2008.

[22] Jones, J., 2000, Contact Mechanics, Cambridge University Press, Cambridge, UK, Chap. 6.